COBEM 2023 27TH INTERNATIONAL CONGRESS OF MECHANICAL ENGENEERING

ABCM Brazilian Society of Mechanical Sciences and Engineering
27th ABCM International Congress of Mechanical Engineering
December 04-08, 2023, Florianópolis-SC, Brazil

COB-2023-1619 Influence of a Magnetic Field Induced by a Conducting Wire on the Flow Patterns and Heat Transfer of a Thermosensitive Ferrofluid Inside a Square Cavity

Luís Henrique Fraga Castro
Taygoara Felamingo de Oliveira
Adriano Possebon Rosa
Energy and Environment Laboratory (LEA)
Department of Mechanical Engineering, Faculty of Techonology, University of Brasília, Brasil
lhcastro@gmail.com, taygoara@unb.br, aprosa@unb.br

Abstract. *In this work, we investigate how an external magnetic field induced by the electric current passing through a conducting wire affects the flow and heat transfer of a thermosensitive ferrofluid in a bottom-heated two-dimensional cavity. We assume an incompressible and laminar flow of a Newtonian ferrofluid whose magnetic susceptibility and density are dependent on the temperature. Under the simultaneous action of the gravitational and external magnetic field, a complex flow develops inside the cavity. We change the intensity of the external magnetic field aiming to understand how the flow field, temperature distribution, and net heat transfer are affected. We use a numerical methodology to solve mass, linear momentum, and energy equations. The pressure-velocity coupling is carried out by a projection method that combines second-order finite differences for spatial discretization, with a Crank-Nicolson scheme for time evolution. The method is verified using results from the literature. Our findings reveal that the magnetic field has a significant influence on the topology of the flow and temperature fields, consequently impacting the overall heat transfer. It is possible to use the magnetic field generated by a conducting wire to change the net heat transfer through the cavity. We found that the Nusselt is a growing function of the magnetic field intensity, except for a specific Rayleigh number. Furthermore, we identify non-stationary regimes at intermediate magnetic Rayleigh numbers, which we attribute to a transition in the flow topology induced by the magnetic field.*

Keywords: *Natural Convection, Ferrofluid, Heat Transfer, Computational Simulation*

1. INTRODUCTION

Ferrofluids are stable suspensions of magnetic particles dispersed in a Newtonian fluid. These particles, with an average diameter of approximately $10\,nm$, are coated with a surfactant layer, which is $2\,nm$ in width (Shliomis, 1974; Rosensweig, 1985). The unique behavior of ferrofluids, which originates from their interaction with external magnetic fields, makes this complex materials very attractive, from a scientific point of view, and leads to many technical applications. For example, ferrofluids has been employed in loudspeaker drivers and accelerometers (Bailey, 1983; Raj and Moskowitz, 1990; Scherer and Figueiredo Neto, 2005), magnetic drug targeting inside of animals and humans to treat diseases (Cole *et al.*, 2011; Lübbe *et al.*, 2001), magnetohyperthermia, a procedure to treat cancer, (Brusentsov *et al.*, 2002; Bubnovskaya *et al.*, 2014; Hiergeist *et al.*, 1999; Guimarães *et al.*, 2020; Obaidat *et al.*, 2015) and cooling of electronic devices (Pattanaik *et al.*, 2021).

An external magnetic field, generated by an electric current running through a conducting wire or a permanent magnet, has the ability to induce or modify the flow of a ferrofluid, and can also alter its viscosity and other rheological properties (Yamaguchi, 2008; Kothari *et al.*, 2010). Additionally, the ferrofluid is a thermosensitive material, meaning that the temperature has a significant influence on its properties, particularly the magnetization, which is the average orientation of the magnetic particles (Jin *et al.*, 2012; Jin and Zhang, 2013), and the density. As a consequence, a magnetic field can influence the natural convection of the ferrofluid, a phenomenon called thermomagnetic convection.

Many authors have investigated the subject of thermomagnetic convection in the last decades, both experimentally (Kikurá *et al.*, 1993; Yamaguchi *et al.*, 2010; Gontijo and Cunha, 2012) and theoretically (Yamaguchi *et al.*, 1999; Snyder *et al.*, 2003; Marcelino *et al.*, 2007; Ashouri *et al.*, 2010; Kefayati, 2014; Selimefendigil *et al.*, 2014; Ashouri and Shafii, 2017; Wada *et al.*, 2020; Cunha *et al.*, 2020; Castro *et al.*, 2022). Wada *et al.* (2020) developed a numerical study, using Lattice-Boltzmann, on the effects of a magnetic field induced by a magnet on the topology of Bénard cells in a rectangular cavity. The results showed that the position and the number of magnets significantly affect the number and the shape of the cells.

Recently, Cunha *et al.* (2020) developed a numerical study on the thermoconvection behavior of a ferrofluid inside a square cavity and under the influence of a linear magnetic field. The investigation was done by a finite element method and results demonstrated the effect on the ferrofluid flow and on the overall heat transfer. Castro *et al.* (2022) investigated,

numerically, the influence of an internal rectangular heated obstacle on the behavior of a ferrofluid inside a square cavity under the influence of an intense magnetic field. They observed that the magnetic field can improve heat transfer and also can lead to a mixture between the fluids in the cold and hot regions of the cavity.

In this work, we investigate the influence of a magnetic field on the flow of a thermosensitive ferrofluid inside a two-dimensional cavity with insulated vertical walls and constant-temperature horizontal walls. The external magnetic field is generated by an electrically conducting wire near the cavity and we consider the ferrofluid's magnetic susceptibility to be temperature-dependent. Our primary objective is to improve the understanding of the complex interactions between magnetic and temperature fields and to explore the implications of this interaction on the overall behavior of the ferrofluid.

2. PROBLEM FORMULATION AND MATHEMATICAL MODEL

We investigate, in this work, the thermomagnetic convection of a ferrofluid in a two-dimensional square cavity of size L, as shown in Fig. 1. The cavity's two vertical walls are insulated ($\dot{Q} = 0$, where $\dot{Q}$ represents the heat transfer rate), while the bottom wall is kept at a constant T_H temperature and the top wall at T_C temperature, with $T_H > T_C$. The gravity acceleration vector, $\mathbf{g}$ is oriented in the negative y axis direction and the magnetic field source, a conducting wire perpendicular to the cavity plane, is placed outside the cavity. The equation for the magnetic field $\mathbf{H}$ is given by

$$\mathbf{H} = \frac{I}{2\pi}\left[\frac{-(y-y_w)\,\hat{\mathbf{e}}_x + (x-x_w)\,\hat{\mathbf{e}}_y}{(x-x_w)^2 + (y-y_w)^2}\right], \tag{1}$$

where x_w and y_w are the coordinates of the wire position and I is the intensity of electric current. In equation 1, $\hat{\mathbf{e}}_x$ and $\hat{\mathbf{e}}_y$ represent the unitary vectors in the x and y axis directions, respectively.

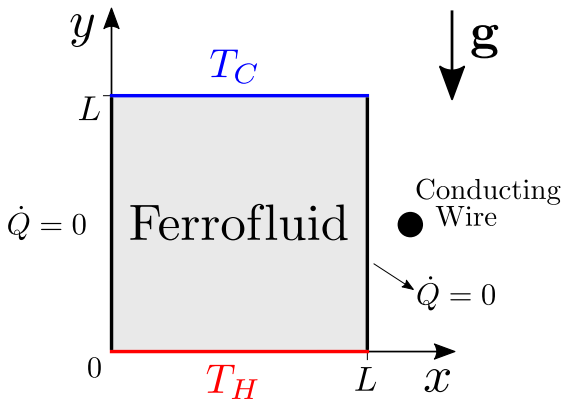

Figure 1: Schematic illustration of the problem investigated in this work. The ferrofluid is inside a square cavity of side length L. The left and right walls are thermally insulated ($\dot{Q} = 0$). The bottom wall is maintained at a constant temperature T_H, while the top wall is held at T_C. The gravity acceleration vector is directed along the negative y-axis, and a conducting wire is positioned close to the cavity.

The ferrofluid is modeled as an incompressible superparamagnetic fluid (Rosensweig, 1985). Its behavior is governed by a modified form of the Navier-Stokes equations, which describe the fluid flow, and the energy conservation equations. The gravitational and magnetic buoyancy forces are mainly associated with thermal effects and are calculated in this work by assuming a Boussinesq approximation. In a non-dimensional form, these equations can be written as

$$\nabla \cdot \mathbf{u} = 0\,, \qquad \frac{\partial \mathbf{u}}{\partial t} + \mathbf{u}\cdot\nabla\mathbf{u} = -\nabla p + \frac{Pr}{(RaPr)^{\frac{1}{2}}}\,\nabla^2\mathbf{u} + \theta\hat{\mathbf{e}}_y - \frac{Ra_m}{Ra}\theta\nabla\left(\frac{H^2}{2}\right) \tag{2}$$

and

$$\frac{\partial \theta}{\partial t} + \mathbf{u}\cdot\nabla\theta = \frac{1}{(RaPr)^{\frac{1}{2}}}\,\nabla^2\theta\,, \tag{3}$$

where t is time, $\mathbf{u}$ is the velocity field, p is pressure, θ is the temperature and H is the magnetic field intensity. We take the local magnetic field to be coincident with the imposed external field, which means that we do not solve the Maxwell equations for the magnetic field. A detailed description of the steps to derive Eq. (2) and Eq. (3) can be found in the paper of Cunha *et al.* (2020) and in Castro (2023).

The non-dimensional parameters that dictates the problem are the Prandtl, Rayleigh and magnetic Rayleigh numbers. The Prandtl number is defined as $Pr = \nu/\alpha$, where ν is the kinematic viscosity and α is the thermal diffusion coefficient.

The Rayleigh number is given by

$$Ra = \frac{g\beta\left(T_H - T_C\right)L^3}{\nu\alpha}, \tag{4}$$

where g is gravitational acceleration intensity and β is volumetric expansion coefficient. The magnetic Rayleigh number is defined by

$$Ra_m = \frac{\mu_0\chi_0\beta_M\left(T_H - T_C\right)H^2L^2}{\eta\alpha}, \tag{5}$$

where μ_0 is the vacuum magnetic permeability, χ_0 is the magnetic susceptibility of the ferrofluid and β_M is the pyromagnetic coefficient (Henjes, 1993).

The calculation of the heat transfer across the cavity for different magnetic field intensities is one of the main goals of this work. The heat transfer is quantified by the average Nusselt number, which can be calculated for the bottom wall,

$$\overline{Nu}_{bottom} = -\int_0^1 \left.\frac{\partial\theta}{\partial y}\right|_{y=0} dx\,, \tag{6}$$

or for the top wall,

$$\overline{Nu}_{top} = -\int_0^1 \left.\frac{\partial\theta}{\partial y}\right|_{y=1} dx\,. \tag{7}$$

The side walls of the cavity are thermally insulated, preventing any thermal energy from entering or leaving through them. The Nusselt number is a non-dimensional parameter that represents the ratio between the total heat flux across a surface and the conductive heat flux through that surface. In a steady-state situation, we have $\overline{Nu}_{bottom} = \overline{Nu}_{top} = \overline{Nu}$ in absolute value. This equality means that the energy entering the cavity through the bottom is equal to the energy leaving it through the top wall.

3. NUMERICAL METHODOLOGY

We employ a second-order projection method, originally proposed by Bell *et al.* (1989) and later improved by Brown *et al.* (2001), to solve the governing equations, namely Eqs. (2) and (3). In the first step, we use the momentum equation to calculate an intermediate velocity field $\mathbf{u}^\star$:

$$\frac{\mathbf{u}^\star - \mathbf{u}^k}{\Delta t} + \left(\mathbf{u}\cdot\nabla\mathbf{u}\right)^{k+\frac{1}{2}} = -\nabla p^{k-\frac{1}{2}} + \frac{Pr}{2\left(RaPr\right)^{\frac{1}{2}}}\nabla^2\left(\mathbf{u}^\star + \mathbf{u}^k\right) + \theta^{k+\frac{1}{2}}\hat{\mathbf{e}}_y - \frac{Ra_m}{Ra}\left(\theta^{k+\frac{1}{2}}\right)\nabla\left[\frac{H^2}{2}\right] \tag{8}$$

and

$$\mathbf{u}^\star = \mathbf{u}_b + \Delta t\nabla\phi^k \quad in \quad \partial\Omega, \tag{9}$$

where k represents the current time-step and $\partial\Omega$, refers to the boundary of the ferrofluid domain, which consists in a square of side 1. To calculate the properties in the intermediate time-step, we use a second-order formula given by $\Psi^{k+\frac{1}{2}} = 2\Psi^k - \Psi^{k-1}$, for a generic Ψ variable. The second step of the method consists on the calculation of the new velocity by

$$\mathbf{u}^{k+1} = \mathbf{u}^\star - \Delta t\nabla\phi^{k+1}\,, \tag{10}$$

where ϕ is a pressure-like auxiliary function calculated by a Poisson equation,

$$\nabla^2\phi^{k+1} = \frac{1}{\Delta t}\nabla\cdot\mathbf{u}^\star \tag{11}$$

and $\nabla\phi^{k+1}\cdot\hat{n} = 0\ in\ \partial\Omega$. The actual pressure is calculated in the third step,

$$p^{k+\frac{1}{2}} = p^{k-\frac{1}{2}} + \phi^{k+1} - \frac{Pr\Delta t}{2\left(RaPr\right)^{\frac{1}{2}}}\nabla^2\phi^{k+1}. \tag{12}$$

Finally, we update the non-dimensional temperature field θ by solving the semi-implicit equation

$$\frac{\theta^{k+1} - \theta^k}{\Delta t} + \mathbf{u}^{k+\frac{1}{2}}\cdot\nabla\theta^{k+\frac{1}{2}} = \frac{1}{2\left(RaPr\right)^{\frac{1}{2}}}\left[\nabla^2\theta^{k+1} + \nabla^2\theta^k\right]. \tag{13}$$

The calculation of the spatial derivatives was performed in a regular and staggered grid by a finite differences approximation. We use a second-order central formulation for all terms, except for the convective ones, for which we use a third order upwind method (Bruneau and Saad, 2006, 2007). The resulting algebraic linear systems of equations are solved by a SSOR preconditioned conjugate gradient method (Saad, 2003). Finally, the code is implemented in Python 3.8 and optimized with the Numba library.

3.1 Mesh Convergence Test and Verification

Table 1 presents a mesh convergence test conducted on the Nusselt number for $Ra = 10^4$ and $Ra_m = 10^5$. We have used a time-step of $\Delta t = 0.1$ and a final time of 1000 for the simulation. The absolute tolerances for the linear system solvers were set as 10^{-5} for the velocity and 10^{-6} for temperature and pressure. It is observed that the difference between the $N = 100$ simulation and the $N = 250$ is 0.2%. Therefore, all the subsequent results in this paper were obtained with $N = 100$.

Table 1: $\overline{Nu}$ as a function of mesh size ($Ra = 10^4$ e $Ra_m = 10^5$).

Mesh Size (N × N)	$\overline{\mathbf{Nu}}$
40×40	3.493
50×50	3.473
60×60	3.459
80×80	3.447
100×100	3.442
150×150	3.438
160×160	3.437
200×200	3.436
250×250	3.435

Our results were also verified by a comparison with other works in the literature. Table 2 shows the Nusselt number (for $Ra_m = 0$ and $Pr = 0.71$) for different values of Ra. Our results can be found to be very similar to those obtained by Davis (1983) and Cunha *et al.* (2020). Figure 2 shows a qualitatively comparison for $Ra = 10^3$ and $Ra_m = 10^6$. We compare the temperature field obtained by this work with that obtained by Cunha *et al.* (2020). Here we have used the same linear magnetic field as in Cunha *et al.* (2020) and also a greater temperature at the top wall. The results show a good agreement between both results.

Table 2: Comparison with $\overline{Nu}$ from Davis (1983) and Cunha *et al.* (2020), for ($Ra_m = 0$).

Ra	$\mathbf{10^3}$	$\mathbf{10^4}$	$\mathbf{10^5}$	$\mathbf{10^6}$
$\overline{Nu}$ (Davis, 1983)	1.118	2.243	4.519	8.800
$\overline{Nu}$ (Cunha *et al.*, 2020)	1.118	2.245	4.522	8.825
$\overline{Nu}$	1.118	2.247	4.538	8.939

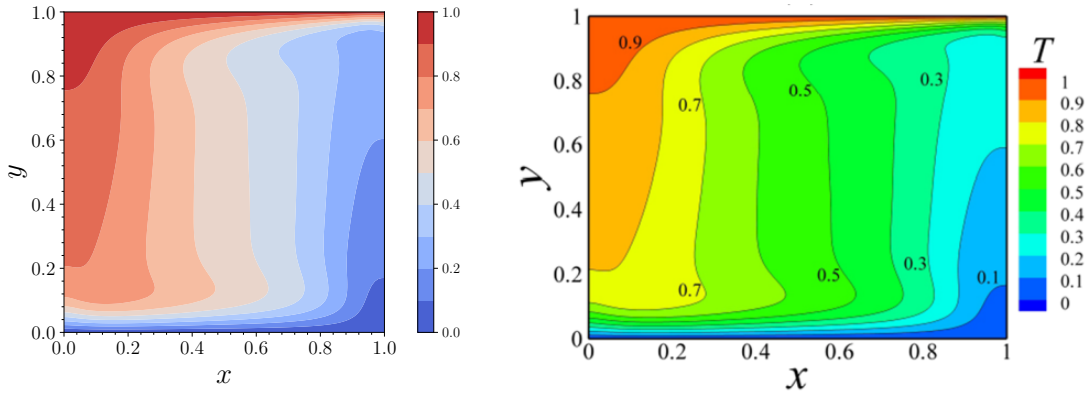

(a) (b)

Figure 2: Comparison of temperature fields generated obtained in the present work (a) and by Cunha *et al.* (2020) (b), for $Ra = 10^3$ and $Ra_m = 10^6$. In this case, the cavity is heated from the top wall, and a linear magnetic field is applied.

4. RESULTS

In this section, we present our results for the ferrofluid behavior inside a square cavity that is heated from the bottom wall. All results here were obtained for $Pr = 100$ and for a conducting wire which is positioned at $(x, y) = (1.05, 0.5)$. The initial condition for the simulations is $\theta = 0$ and $u = v = 0$ inside the domain.

Figure 3 presents the temperature field and the streamlines for $Ra = 10^3$. For the zero magnetic case, shown in Fig. (a), the temperature difference between the top and bottom plates is not enough to start the flow. In this case, the fluid remains stationary and the heat is transferred only by conduction, which results in a linear temperature distribution and $\overline{Nu} = 1$. For infinitely long parallel plates, the critical Ra number for which the flow starts is calculated as 1708 (Bejan, 2013). This is in fact what we observe in Fig. (a), since the Ra is smaller than the critical value in this case.

Figure 3 (b) shows the result when a magnetic field, corresponding to $Ra_m = 10^4$, is applied to the ferrofluid. The magnetic field exerts an attractive influence on the magnetic particles within the ferrofluid, giving rise to a magnetic force directed towards the location of the conducting wire. This force is directly related to the local magnetization of the ferrofluid, which, in turn, exhibits an inverse relationship with temperature. Consequently, the cold fluid exhibits a greater attraction towards the magnetic field source compared to the hot fluid. From the streamlines in Fig. 3 (b), we can observe that the wire pulls the fluid at the top of the cavity, which is at a lower temperature, and creates a big circular flow in the cavity. The temperature convection breaks the linear configuration shown in Fig. 3 (a), since the flow carries the thermal energy with itself. As a consequence, the enhanced fluid flow caused by the magnetic force results in an increased heat transfer across the cavity. In this particular case, the average Nusselt number ($\overline{Nu}$) reaches a value of 1.490, indicating the improved heat transfer efficiency.

An increase in the magnetic field magnitude leads to a more intense flow, as shown by Figs. 3 (c) and 3 (d), with $Ra_m = 10^5$ and $Ra_m = 10^6$, respectively. The flow carries the hot fluid towards the top plates, on the left side of the cavity and, simultaneously, transport cold fluid to the cavity bottom through the region close to the right wall. The center of the recirculation zone moves to the top right of the cavity. Also, the topology of the flow becomes more complex for the greater magnetic field. The intensity of the velocity is significantly increased by the magnetic field, as shown by Figs. 4 (a) and (b). The maximum velocity is located in the top right region of the cavity, where the conducting wire exerts its attractive force. These changes in velocity and temperature field lead to an increase in the average Nusselt number, which is calculated as 2.427 for $Ra_m = 10^5$ and 4.144 for $Ra_m = 10^6$.

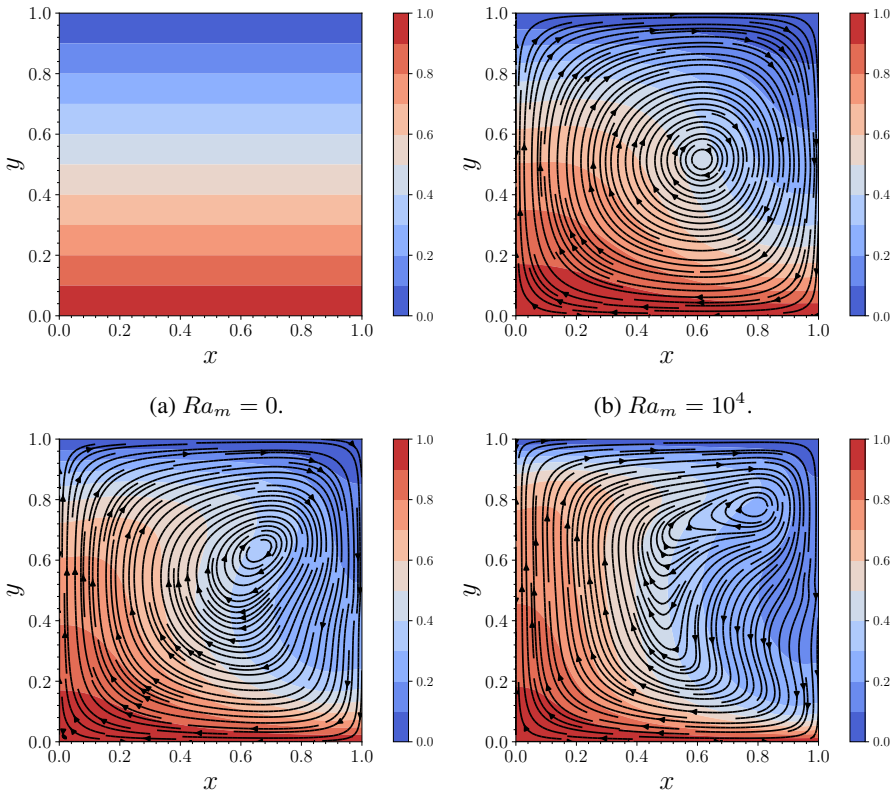

(a) $Ra_m = 0$. (b) $Ra_m = 10^4$.

(c) $Ra_m = 10^5$. (d) $Ra_m = 10^6$.

Figure 3: Temperature field and streamlines for $Ra = 10^3$. The magnetic field is generated by a conducting wire perpendicular to the cavity plane and positioned at $x = 1.05$ and $y = 0.5$.

Changing from $Ra = 10^3$ to $Ra = 10^4$, in figure 5, we observe some distinctions in both the fluid flow patterns and temperature distribution. First, the temperature difference between the bottom and top walls are large enough to start the fluid flow inside the cavity, as can be observed in Fig. 5 (a). The hot fluid from the bottom wall rises through the left side of the cavity, while the denser cold fluid descends close to the right wall. We can observe a good mixture of the hot and cold regions throughout the cavity, which results in a Nusselt number $\overline{Nu} = 2.194$ in this situation. When a magnetic

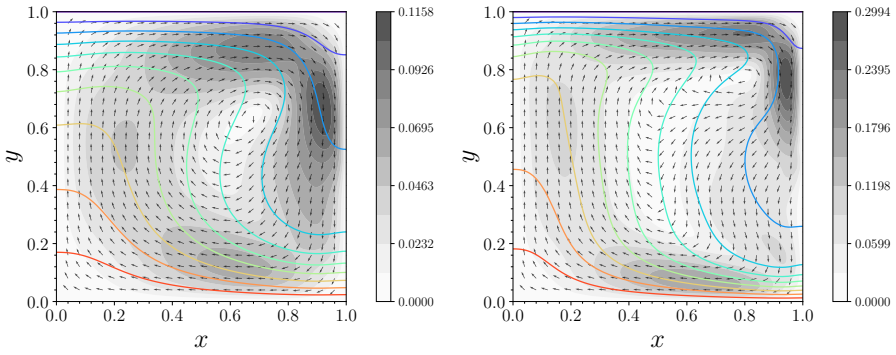

(a) $Ra_m = 10^5$. (b) $Ra_m = 10^6$.

Figure 4: Velocity intensity and direction for $Ra = 10^3$. Arrows indicate velocity direction, and gray colors represent its magnitude. Colored lines depict the temperature field.

field corresponding to $Ra_m = 10^4$ is imposed, we observe almost no changes in the ferrofluid behavior, as show in Fig. 5 (b). In this case we have $Ra_m < Ra$, which means that the thermal contribution dominates the problem and that the magnetic force is of little importance to the problem. This was also observed by Cunha *et al.* (2020): the magnetic field affects the flow for Ra_m greater or at least of the same order of Ra. Still, the magnetic field helps the thermal buoyancy and the result is a small increase in the Nusselt number in this case, with $\overline{Nu} = 2.327$.

Figure 5 (c) shows the result for $Ra = 10^4$ and $Ra_m = 10^5$. In this case we observe a change in the streamlines, with its center moving from the center of the cavity in the top-right direction. The Nusselt number for this case is 2.849, which shows a more significant variation. Figure 5 (d) shows the result for $Ra_m = 10^6$. In this case, the magnetic force dominates the thermal buoyancy effect and the topology of the flow is modified from the $Ra_m = 10^5$ situation. This result is actually quite similar to the one shown by Fig. 3 (d). We can conclude that the magnetic force is dominant in this situation and the ferrofluid behavior is governed by its configuration. In fact, the Nusselt numbers are very close, with $\overline{Nu} = 4.331$ for $Ra = 10^4$ and $Ra_m = 10^6$, in comparison with $\overline{Nu} = 4.144$ for $Ra = 10^3$ and $Ra_m = 10^6$.

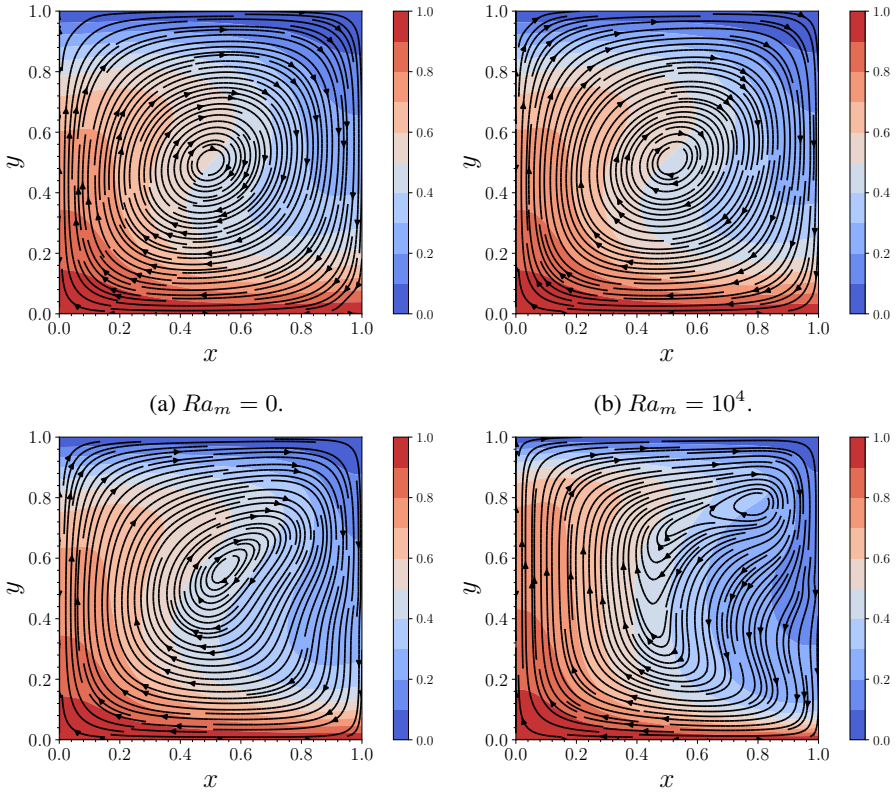

(a) $Ra_m = 0$. (b) $Ra_m = 10^4$.

(c) $Ra_m = 10^5$. (d) $Ra_m = 10^6$.

Figure 5: Temperature field and streamlines for $Ra = 10^4$. The magnetic field is generated by a conducting wire perpendicular to the cavity plane and positioned at $x = 1.05$ and $y = 0.5$.

For $Ra = 10^5$, a notable change in the behavior of the ferrofluid is observed, as shown by Fig. 6. First, there is an intensification of the gravitational buoyancy within the cavity, to the point of generating two zones of recirculation, rotating in opposite directions, as shown in (a). This configuration represents the Bénard cells (Bénard, 1900) that spontaneously appear in problems of natural convection. The heat transfer is intensified by the formation of the cells, which results in a Nusselt number $\overline{Nu} = 4.169$. Another important characteristic to emphasize is that this Bénard cell configuration causes the low-temperature ferrofluid to flow downwards through the center of the cavity, while the high-temperature ferrofluid flows upwards through the cavity's sides.

A conducting wire positioned in $x = 1.05$ and $y = 0.5$ will induce an attraction on the colder fluid, pulling it towards its direction. This force acts against the flow direction depicted in Fig. 6 (a). As a result, the magnetic field breaks the Bénard cells, Fig. 6 (b), and restores the previous single-circulating zone configuration as observed for smaller Ra numbers. There is a intense mixture of the hot and cold fluid at the cavity's center. The calculated Nusselt number for this case is 3.890, which is smaller than the zero magnetic field case. The reason for this result is that the two Bénard cells formation is more effective is taking the heat from the hot wall and transmitting it to the cold wall. When the magnetic field breaks the cells and make them one, there is a reduction in the overall heat transfer across the cavity. Increasing the Ra_m to 10^6 leads to small changes in the streamlines and temperature fields, as shown in Fig. 6 (c). The Nusselt number for this case, 4.030, is still below the case with no magnetic field. These results shows that the magnetic field can in fact hinder the heat transfer by changing the flow topology. The last result, for $Ra_m = 10^6$, is shown in Fig. 6 (d). In this case the magnetic field induces significant changes in the streamlines format and the result is an increase in the calculated Nusselt number to $Nu = 5.059$.

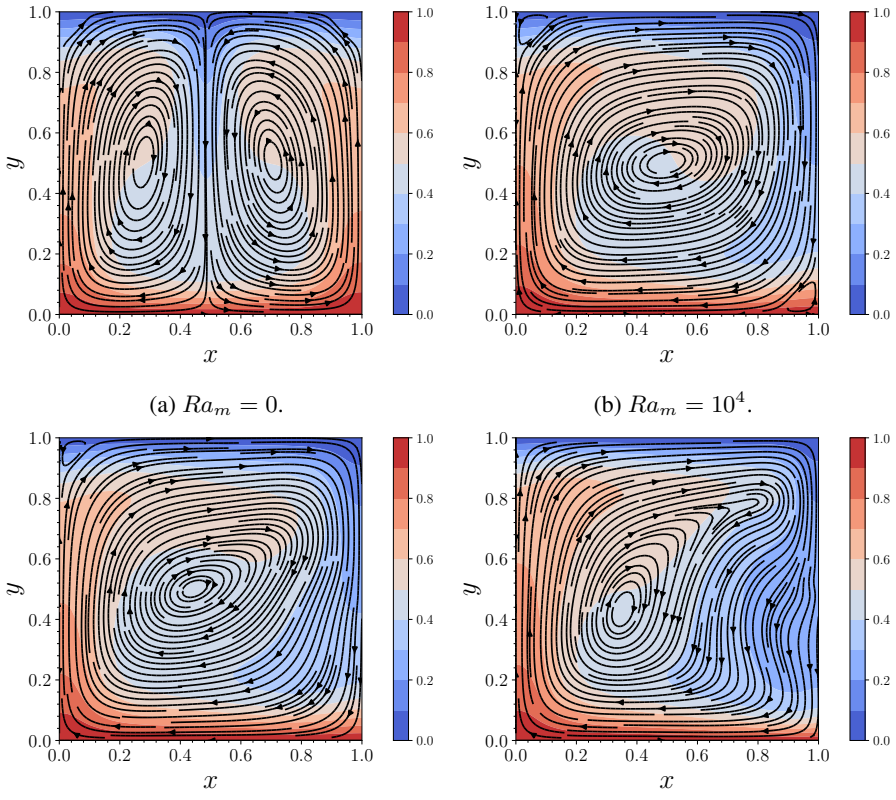

(a) $Ra_m = 0$. (b) $Ra_m = 10^4$.

(c) $Ra_m = 10^5$. (d) $Ra_m = 10^6$.

Figure 6: Temperature field and streamlines for $Ra = 10^5$. The magnetic field is generated by a conducting wire perpendicular to the cavity plane and positioned at $x = 1.05$ and $y = 0.5$.

A compilation of the previous results is presented in Fig. 7, which shows the influence of the magnetic Rayleigh number Ra_m on the Nusselt number $\overline{Nu}$, for $Ra = 10^3$, $Ra = 10^4$ and $Ra = 10^5$. In the interval shown in the figure, for $Ra = 10^3$ and $Ra = 10^4$, we can observe that the magnetic field imposed increases the heat transfer, since it intensifies the velocity field and contributes to a better mixture of the hot and cold fluids. For high values of Ra_m, the magnetic force dominates the ferrofluid behavior and the Nusselt number seems to converge to the same value. H

The behavior for $Ra = 10^5$ is quite different and more complex. First, for $Ra_m = 0$, we observe two Bénard cells and a calculated $\overline{Nu} = 4.169$. For $Ra_m = 10^4$, the magnetic field break the cells and we have a big circulation zone. For greater values of Ra_m the $\overline{Nu}$ increases. However, for Ra_m of 10^2 and 10^3 we encountered an unexpected behavior: the magnetic field disturbs the original Bénard cells but it is not strong enough to take the flow to one cell only. In this

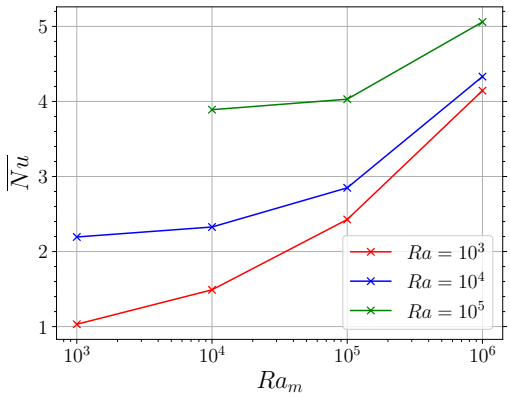

Figure 7: Calculated Nusselt number as a function of Ra_m for $Ra = 10^3$, 10^4 and 10^5.

case, the flow does not reach a stationary solution and keeps oscillating. Figure 8 shows $\overline{Nu}$ as a function of time for $Ra = 10^5$ and different values of Ra_m. For $Ra_m = 0$ we can observe a transient period an then the flow reaches a permanent configuration. The same trend is depicted by the situation for $Ra_m = 10^4$. The $Ra_m = 10^2$ and $Ra_m = 10^3$ simulations show a different behavior. For these parameters, $\overline{Nu}$ does not reach an stationary value, but keeps oscillating. For the period of time investigated, these oscillations seem to be regular, with a constant frequency. Figure 9 (a) shows the temperature distribution and the streamlines for $Ra = 10^5$ and $Ra_m = 10^2$, while Fig. 9 (b) shows for $Ra = 10^5$ and $Ra_m = 10^3$, both at time $t = 3000$. It is possible to notice a significant recirculation zone in the bottom-left side of the cavity. This recirculation zone exhibits a dynamic behavior, expanding and contracting repeatedly over time. Although we have not fully understood this phenomenon yet, we are actively working on gaining a better understanding of it.

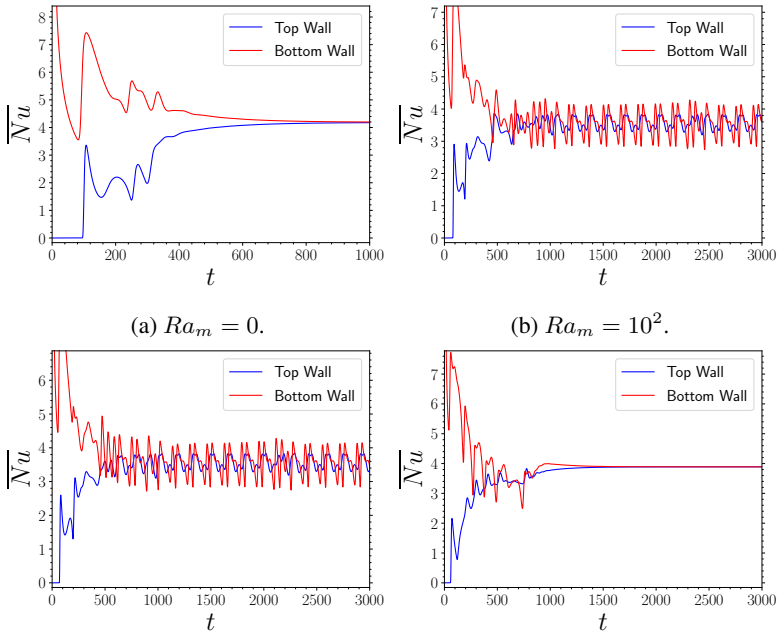

(a) $Ra_m = 0$. (b) $Ra_m = 10^2$.

(c) $Ra_m = 10^3$. (d) $Ra_m = 10^4$.

Figure 8: Nusselt number $\overline{Nu}$ as a function of time for $Ra = 10^5$ and different values of Ra_m.

5. CONCLUSIONS

In this study, we investigated the influence of a magnetic field generated by a conducting wire on the behavior of a ferrofluid inside a bottom-heated square cavity. Our findings demonstrate that the magnetic force plays a crucial role in initiating the flow when the temperature difference is insufficient. The induced flow significantly enhances the heat across the cavity. It was found that the magnetic field increases the velocity of the fluid and can change the flow topology when the magnetic Rayleigh number exceeds the Rayleigh number. For the case of $Ra = 10^5$, we observed the formation of two Bénard cells for the zero magnetic field case. However, these cells are brought back to a single one by the magnetic field, resulting in a decrease of the Nusselt number for intermediary values of Ra_m. Additionally, our study revealed non-

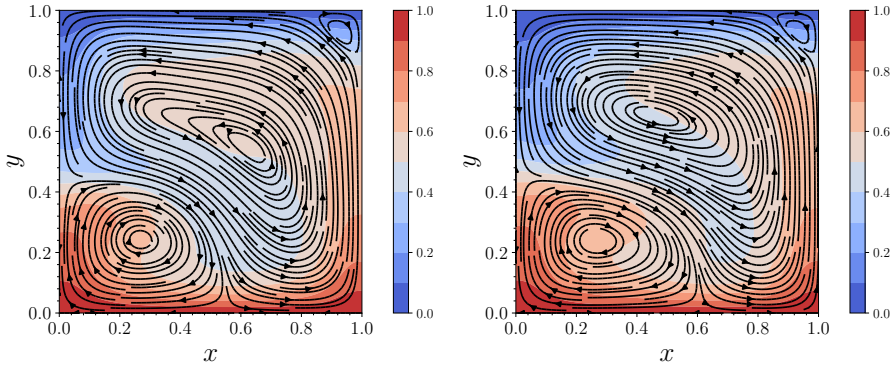

(a) $Ra_m = 10^2$. (b) $Ra_m = 10^3$.

Figure 9: Temperature field and streamlines for the non-stationary cases. $Ra = 10^5$ and $t = 3000$.

stationary behavior for $Ra_m = 10^2$ and 10^3, when $Ra = 10^5$. For these values of the magnetic field, the Nusselt number fails to reach an equilibrium value. In our future work, we will investigate in more details the underlying mechanisms behind the observed non-stationary behavior, conducting a comprehensive research to further elucidate the dynamics of this phenomenon.

6. REFERENCES

Ashouri, M., Ebrahimi, B., Shafii, M.B., Saidi, M.H. and Saidi, M.S., 2010. "Correlation of nusselt number in pure magnetic convection ferrofluid flow in a square cavity by a numerical investigation". *Journal of Magnetism and Magnetic Materials*, Vol. 322, pp. 3607–3613.

Ashouri, M. and Shafii, M.B., 2017. "Numerical simulation of magnetic convection ferrofluid flow in a permanent magnet-inserted cavity". *Journal of Magnetism and Magnetic Materials*, Vol. 422, pp. 270–278.

Bailey, R.L., 1983. "Lesser known applications of ferrofluid". *Journal of Magnetism and Magnetic Materials*, Vol. 39, pp. 178–182.

Bejan, A., 2013. *Convection Heat Transfer*. John Wiley & Sons, Inc.

Bell, J.B., Colella, P. and Glaz, H.M., 1989. "A second-order projection method for the incompressible navier-stokes equation". *Journal of Computational Physics*, Vol. 85, pp. 257–283.

Brown, D., Cortez, R. and Minion, M., 2001. "Accurate projection methods for the incompressible navier-stokes equation". *Journal of Computational Physics*, Vol. 198, pp. 464–499.

Bruneau, C.H. and Saad, M., 2006. "The 2d lid-driven cavity problem revisited". *Computational Fluid Dynamics Journal*, Vol. 35, pp. 326–348.

Bruneau, C.H. and Saad, M., 2007. "The behavior of high reynolds flows in a driven cavity". *Computational Fluid Dynamics Journal*, Vol. 15.3, pp. 1–11.

Brusentsov, N.A., Nikitin, V., Brusentsova, T.N., Kuznetsov, A.A., Bayburtskiy, F.S., Shumakov, L.I. and Jurchenko, N.Y., 2002. "Magnetic fluid hyperthermia of the mouse experimental tumor". *Journal of Surgical Research*, Vol. 252, pp. 378–380.

Bubnovskaya, L., Belous, A., Solopan, S., Kovelskaya, A., Bovkun, L., Podoltsev, A., Kondtratenko, I. and Osinsky, S., 2014. "Magnetic fluid hyperthermia of rodent tumors using manganese perovskite nanoparticles". *Journal of Nanoparticles*, Vol. 278761, pp. 1–9.

Bénard, M.H., 1900. "Étude expérimentale des courants de convection dans une nappe liquide - régime permanent: Tourbillons cellulaires". *Journal de Physique Théorique et Appliquée*, Vol. 9, pp. 513–524.

Castro, L.H.F., Cunha, F.R. and Rosa, A.P., 2022. "Convecção termomagnética em uma cavidade quadrada com obstáculo interno aquecido: uma investigação numérica". In *Proceedings of the XV Congreso Iberoamericano de Ingeniaría Mecánica - CIBIM 2022*. Departamento de Ingeniaría Mecánica - Universidad Politécnica de Madri, Universidad Politécnica de Madri, Madrid, Spain.

Castro, L.H.F., 2023. *Numerical Study of Magnetic Thermoconvection in a Cavity(in Portuguese)*. Master's thesis, Graduate Program in Mechanical Sciences, Federal University of Brasília, Brasília, Brasil.

Cole, A.J., Yang, V.C. and David, A.E., 2011. "Cancer theranostics: The rise of targeted magnetic nanoparticles". *Trends in Biotechnology*, Vol. 29, pp. 323–332.

Cunha, L.H.P., Siqueira, I.R., Campos, A.A.R., Rosa, A.P. and Oliveira, T.F., 2020. "A numerical study on heat transfer of a ferrofluid flow in a square cavity under simultaneous gravitational and magnetic convection". *Theoretical and Computational Fluid Dynamic*, pp. 1–15.

Davis, G.V., 1983. "Natural convection of air in a square cavity: a bench mark numerical solution". *International Journal*

for Numerical Methods in Fluids, Vol. 3, pp. 249–264.

Gontijo, R.G. and Cunha, F.R., 2012. "Experimental investigation on thermo-magnetic convection inside cavities". *Journal of Nanoscience and Nanotechnology*, Vol. 12, pp. 9198–9207.

Guimarães, A.B., Cunha, F.R. and Gontijo, R.G., 2020. "The influence of hydrodynamics effects on the complex susceptibility response of magnetic fluidos undergoing oscillatory fields: New insights for magnetic hyperthermia". *Phys. Fluids*, Vol. 32, pp. 1–18.

Henjes, K., 1993. "Buoyancy forces in magnetic fluids". *Zeitschrift Fur Physik B*, Vol. 92, pp. 113–127.

Hiergeist, R., Andra, W., Buske, N., Hert, R., Hilger, I., Richter, U. and Kaiser, W., 1999. "Application of magnetite ferrofluids for hyperthermia". *Journal of Magnetism and Magnetic Materials*, Vol. 201, pp. 420–422.

Jin, L. and Zhang, X., 2013. "Analysis of temperature-sensitive magnetic fluids in a porous square cavity depending on different porosity and darcy number". *Applied Thermal Engineering*, Vol. 50, pp. 1–11.

Jin, L., Zhang, X. and Niu, X., 2012. "Lattice boltzmann simulation for temperature-sensitive magnetic fluids in a porous square cavity". *Journal of Magnetism and Magnetic Materials*, Vol. 324, pp. 44–51.

Kefayati, G.H.R., 2014. "Natural convection of ferrofluid in a linearly heated cavity utilizing lbm". *Journal of Molecular Liquids*, Vol. 191, pp. 1–9.

Kikurá, H., Sawada, T.S. and Tanahashi, T., 1993. "Natural convection of a magnetic fluid in a cubic enclosure". *Journal of Magnetism and Magnetic Materials*, Vol. 122, pp. 315–318.

Kothari, N., Raina, B., Chandak, K., Iyer, V. and Mahajan, H., 2010. "Application of ferrofluid of enhanced surfactant flooding in eor". *Society of Petroleum Engineers*, Vol. SPE 131272, pp. 1–7.

Lübbe, A.S., Alexiou, C. and Bergemann, C., 2001. "Clinical applications of magnetic drug targeting". *Journal of Surgical Research*, Vol. 95, pp. 200–206.

Marcelino, N.B., Couto, H.L.G. and Cunha, F.R., 2007. "A stury on magnetic convection in a narrow rectangular cavity". *Magnetohydrodynamics*, Vol. 43, pp. 421–328.

Obaidat, I.M., Issa, B. and Haik, Y., 2015. "Magnetic properties of magnetic nanoparticles for efficient hyperthermia". *Nanomaterials*, Vol. 5, pp. 63–89.

Pattanaik, M.S., Varma, V.B., Cheekati, S.K., Chaudhary, V. and Ramanujan, R.V., 2021. "Optimal ferrofluids for magnetic cooling devices". *Scientific Reports*, pp. 1–20.

Raj, K. and Moskowitz, R., 1990. "Commercial applications of ferrofluids". *Journal of Magnetism and Magnetic Materials*, Vol. 85, pp. 233–245.

Rosensweig, R.E., 1985. *Ferrohydrodynamics*. DOVER PUBLICATIONS, INC., Mineola, New York.

Saad, Y., 2003. Iterative Methods for Sparse Linear Systems Society for Industrial and Applied Mathematics.

Scherer, C. and Figueiredo Neto, A.M., 2005. "Ferrofluids: Properties and applications". *Brazilian Journal of Physics*, Vol. 35, pp. 718–727.

Selimefendigil, F., Oztop, H.F. and Al-Salem, K., 2014. "Natural convection of ferrofluids in partially heated square enclosures". *Journal of Magnetism and Magnetic Materials*, Vol. 372, pp. 122–133.

Shliomis, M.I., 1974. "Magnetic fluids". *Soviet Physics Uspekhi*, Vol. 17, pp. 427–458.

Snyder, S.M., Cader, T. and Finlayson, B.A., 2003. "Finite element model of magnetoconvection of a ferrofluid". *Journal of Magnetism and Magnetic Materials*, Vol. 262, pp. 269–279.

Wada, K., Kaneda, M. and Suga, K., 2020. "Rayleigh-bénard convection of paramagnetic liquid under a magnetic field from permanent magnets". *Symmetry*, Vol. 341, pp. 1–11.

Yamaguchi, H., 2008. *Engineering Fluid Mechanics*. Springer.

Yamaguchi, H., Kobori, I. and Uehata, Y., 1999. "Heat transfer in natural convection of a magnetic fluid". *Journal of Thermophysics and Heat Transfer*, Vol. 13, pp. 501–507.

Yamaguchi, H., Zhang, X.R., Niu, X.D. and Yoshikawa, K., 2010. "Thermomagnetic natural convection of thermosensitive magnetic fluids in cubic cavity with heat generating object inside". *Journal of Magnetism and Magnetic Materials*, Vol. 0304-8853, pp. 698–704.

7. RESPONSIBILITY NOTICE

The authors are solely responsible for the printed material included in this paper.